Geotechnical Aspects of Underground Construction in Soft Ground – Ng, Huang & Liu (eds)
© 2009 Taylor & Francis Group, London, ISBN 978-0-415-48475-6

Experimental studies of a geological measuring system for tunnel with ultrasonic transducer

D.H. Kim, U.Y. Kim, S.P. Lee & H.Y. Lee
GS Engineering & Construction, Seoul, Korea

J.S. Lee
Korea University, Seoul, Korea

ABSTRACT: Predicting ground conditions ahead of the tunnel face has been one of the most important requirements of tunnel construction. This study investigated the development and application of a high resolution ultrasonic wave imaging system, which captures the multiple reflections of ultrasonic waves at the interface, to detect discontinuities at laboratory scale rock mass model. Ultrasonic wave reflection imaging based on A- and B-modes was obtained through stacking, signal compensation, demodulation, and display. Experiments were carried out by using horizontal scanning and rotational scanning. Experimental studies showed that the rotational scanning method was able to identify horizontal and inclined discontinuities and the cavity on the plaster block at a fixed location. Furthermore, two discontinuities including horizontal and inclined discontinuity planes were detected. The rotating scanning technique produced images similar to those obtained by the typical horizontal scanning technique. This paper contains basic theories about the ultrasonic transducer and several experimental application results. The full-scale field application and other application will be scheduled in the future.

1 INTRODUCTION

With the rapid growth of the world's population and economics, increasing number of tunnels have been constructed to provide better transport links. Safe and economic tunneling has always been a challenging topic in tunnel construction because of complex ground conditions like faults, fractures, caverns, and wet layers. Therefore, the prediction of ground conditions ahead of tunnel face is considered one of the important requirements.

Many techniques to predict the ground condition ahead of the advancing tunnel face have been developed, improved and widely applied in tunnel construction projects. Three types of techniques are representives for tunnel ground condition predicting: coring, displacement monitoring and analysis, and wave-based non-destructive evaluations(Figure 1(a)).

In this study, a new high resolution seismic technique based on rotating scanning equipment is introduced to detect geological discontinuities, as shown in Figure 1(b). This technique uses the received time series which captures multiple reflections due to the impedance mismatch at a geological interface. The source and receiver transducers are located on the tunnel face at one fixed point. As a preliminary study of this technique, this paper describes experimental studies carried out on lab-scaled models. This paper

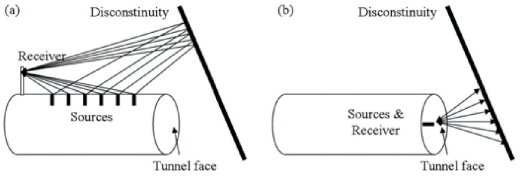

Figure 1. Seismic method for predicting tunnel face: (a) TSP method; (b) Rotating scanning method.

presents basic theories about the ultrasonic transducer including transducer frequency characteristics, transducer beam characteristics, and coupling layer characteristics, experimental setup and signal processing, application examples, discussion, and conclusions.

2 ULTRASONIC TRANSDUCER

Ultrasonic wave reflection imaging system may be an economical and effective tool for the forecast of the ground condition ahead of the tunnel face. A transducer refers to any device that can convert an electrical signal into a mechanical energy and vice versa. In ultrasonic reflection imaging, a piezoelectric lead-zirconate-titanate (PZT) type transducer is generally used to as a source and detector (Wells, 1977). The selection of the transducer is the most important factor

in ultrasonic reflection imaging because the transducer determines the image resolution and skin depth.

2.1 *Transducer frequency characteristics*

The choice of transducer frequency in ultrasonic reflection imaging is the result of a compromise between the resolution (lateral and axial) requirement and the acquirement of satisfactory beam penetration for the imaging of the part of interest. Lateral resolution refers to the ability to distinguish two closely spaced reflectors, which are positioned perpendicular to the axis of the ultrasound beam. Lateral resolution is most closely related to the transducer beamwidth. Axial resolution refers to the minimum reflector spacing along the axis of an ultrasonic beam that results in separate, distinguishable echoes on the display.

For a given frequency, the shorter the pulse duration, the wider the frequency bandwidth. If a shorter pulse duration is used, high resolution can be attained, but it lowers the sensitivity and skin depth. But sensitivity can be improved by either increasing the energy of the transmitter or by amplifying the captured signals at the receiver. Note, skin depth is the ability to detect an anomaly at a given depth and it depends on the amplitude of the reflected signal. When the resolution increases with increasing frequency, the skin depth decreases (Lee and Santamarina 2005).

2.2 *Transducer beam characteristics*

Near Field and Far Field. The transducer beam is characterized as near field and far field, which are sketched in Figure 2. In the near field, which is called the Fresnel zone, wave amplitude fluctuates. Note the beams are almost parallel rather than divergent in the near field. The near field length NFL or Fresnel zone length is dependent on the transducer radius r and wavelength λ (Krautkramer and Krautkramer, 1990; Rose, 1999).

$$NFL \approx \frac{\gamma^2}{\lambda} = \frac{r^2 f}{V} \tag{1}$$

where f is the frequency, and V is the ultrasonic wave velocity of the medium. Therefore, the near field length NFL increases with the increase of the transducer radius r and/or the increase of the frequency f. The zone beyond the near field is the far field, which is also called the Fraunhofer zone. The divergence angle depends on the directivity.

Directivity. The far field divergence angle depends on the wavelength and radius r (or diameter d) of the transducer (Zagzebski, 1996), as shown in Figure 2.

$$\sin\theta = \frac{1.2\lambda}{d} = 1.2\frac{V}{fd} \tag{2}$$

The divergence angle should be made small to increase lateral resolution. Higher frequency and larger diameter render higher lateral resolution (far field is assumed).

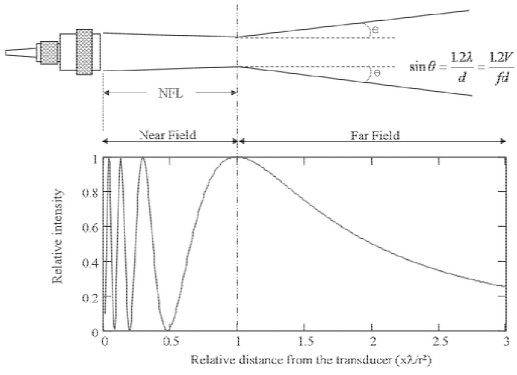

Figure 2. Beam characteristics of transducer.

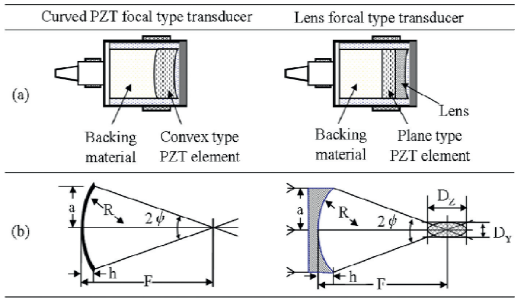

Figure 3. Transducer type and focal length: (a) Schematic drawing of transducer; (b) Focal length.

The directivity of the transducer is affected by the velocity of the test medium, and the frequency and size of the transducer. High directivity yields higher resolution. The directivity of an ultrasonic beam may be altered by focusing the beam: 1) a curved PZT element instead of a plane PZT element is used and 2) a lens is attached in front of the plane PZT element (Schmerr, 1998), as shown in Figure 3. Because the wave velocity in lens is greater than that in water, the shape of the lens will be concave. The focal length F is defined as the distance from the point on the curved surface on the central axis to the midpoint of the region of convergence. Note, if the lens is used, the focal zone instead of the focal point appears, as shown in Figure 3(b). The focal length is dependent on the radius of curvature R, the radius of the lens a, and the aperture angle 2ψ (see Figure 3).

For the investigation of the directivity, two types of transducers are used: focal type transducer (Panametrics A3441) and non-focal transducer (Panametrics V318). Both are high damping immersion transducers having 500 kHz in resonant frequency and 19 mm in diameter. Directivities were investigated by measuring the amplitude of the signal at fixed axial distances (50 mm, 100 mm and 150 mm) and the lateral offsets of the transducers, as shown in Figure 4(a). A focal

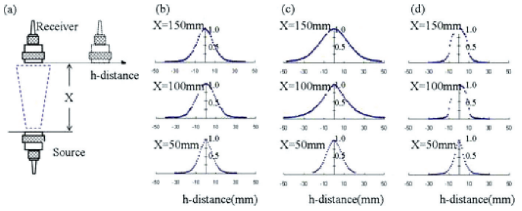

Figure 4. Directivity: (a) Test procedures; (b) Focal type transducer; (c) Non-focal transducer; (d) Lens focal type transducer.

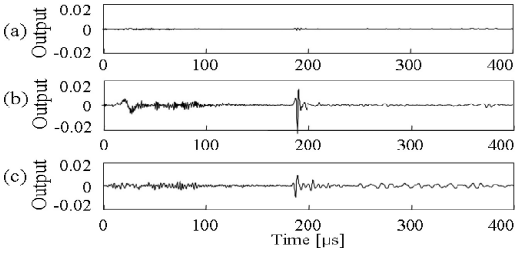

Figure 5. Coupling layer effects: (a) Vacuum grease-not adhered tightly; (b) Vacuum grease-adhered tightly; (c) Water.

type transducer has good directivity, as shown in Figure 4(b). Whereas a non-focal type transducer diverges much of the energy, as shown in Figure 4(c), a non-focal type transducer with a concave lens (lens focal type transducer) improves the directivity dramatically, as shown in Figure 4(d).

Coupling layer characteristics. The coupling layer, which is an agent between transducer and medium, should minimize the reflection from the surface of the medium tested to maximize the energy transferred to the medium. Vacuum grease and water were examined as agents in this study. The test medium was a plaster block of 300 mm in height, 300 mm in width and 150 mm in thickness. The minor energy was reflected with vacuum grease when the transducers were lightly placed on the top of the vacuum grease (it is not adhered tightly), as shown in Figure 5(a). However, when the transducers were tightly adhered, the amplitude of the reflected signal increased, as shown in Figure 5(b). Note, the amplitude of the directly transmitted wave, which propagates from the source to the receiver through the tested medium, also increases. Furthermore, it is very difficult to maintain the constant contact between the transducer and the vacuum grease during the scanning. When water was used as a coupling layer, it produced a relatively high amplitude reflection as shown in Figure 5(c). In addition, the directly transmitted wave can be effectively shielded by using several layers of aluminum foil. Therefore, water was selected as the coupling layer for scanning in this study.

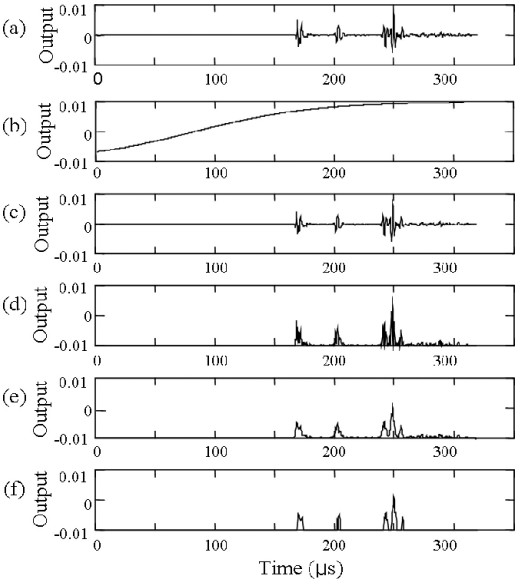

Figure 6. Signal processing: (a) Measured signal after stacking; (b) logsig function(window function) for time gain compensation; (c) Compensated signal; (d) Rectification; (e) Moving averaging; (f) Rejection.

3 EXPERIMENTAL SETUP AND SIGNAL PROCESSING

3.1 *Experimental setup*

A Pulser (JSR, DPR300) was used to generate the ultrasonic waves through the transducer (Panametrics A3441). Two transducers were used as the source and receiver, respectively. The reflected signals due to the impedance mismatch at the interface were detected and converted into electrical signal by the receiver transducer. The electrical signal was fed through an amplifier (Krohn-Hite 3945: frequency range from 170 Hz to 26.5 MHz) because the amplitude of the signals measured by the receiver was generally too low to identify the meaningful reflection. The amplified signal was digitized in the oscilloscope (Agilent 54624A or National Instruments PXI-5112).

3.2 *Signal processing*

Signal processing for ultrasonic imaging consists of stacking, signal compensation, demodulation including rectification and smoothing, rejection, and display (Zagzebski 1996).

Stacking. Signals were captured after stacking, which is the most effective signal processing technique for removing the high frequency, uncorrelated noise. The stacking means averaging multiple signals. The 1024 signals were averaged to obtain the signal trace, as shown Figure 6(a).

Signal compensation. The amplitude of the reflected signals at the receiver generally decreases as the distance of the interfaces, which the waves are reflected from, increases due to the geometrical spreading under identical impedance mismatch. This attenuation may be compensated by using time gain compensation (TGC), which increases the amplitude with time. Thus, the amplification factor is higher at a longer distance than at a shorter distance from the receiver. In this study, the adopted TGC is a log sigmoid (logsig) transfer function, as shown in Figure 6(b). The compensated signal is obtained through point-by-point multiplication between the original signal and logsig function. Figure 6(c) shows the compensated signal from the original signal. The amplitude of the first and second reflections decreases.

Demodulation. Demodulation includes rectification and smoothing. Rectification is an inversion of negative components. Thus, the signal has only positive values, as shown in Figure 6(d). Smoothing (moving average) was carried out by using the kernel of [1/20, 2/20, 4/20, 6/20, 4/20, 2/20, 1/20] in this study. The signal after the smoothing process is shown in Figure 6(e).

Rejection. Rejection is an elimination process, which removes the signal whose amplitude is less than threshold value. Thus, rejection removes noises and low amplitude signals. In this study, the threshold value was about 20% of the maximum amplitude. The signal after rejection is shown in Figure 6(f).

Display. Two modes were used to display the ultrasonic reflection imaging in this study. First, the amplitude mode (A-mode), which represents the amplitude of the signal after rejection versus time, was used. In the A-mode, the first arrival time of the reflected signal can be easily determined. Note the height of the trace in the A-mode is the amplitude. Second, the amplitude of each signal was converted to brightness, which is proportional to the amplitude of the reflected signal. The brightness versus time is the brightness mode (B-mode).

4 APPLICATION EXAMPLES

Several unique applications of ultrasonic wave monitoring and imaging were explored by using several small scale plaster blocks and one large scale plaster block.

4.1 *Rotating scanning test for the small scale plaster blocks*

Three kinds of specimens were used for the rotating scanning tests: an intact plaster block, a plaster block with an inclined crack, and a plaster block with a cavity. The dimensions of the plaster block were 300 mm in height, 300 mm in width and 150 mm in thickness. The middle of the top surface of the plaster block was dug

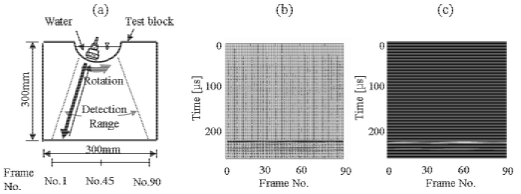

Figure 7. Rotating scanning test for an intact plaster block: (a) Test setup; (b) A-mode image; (c) B-mode image.

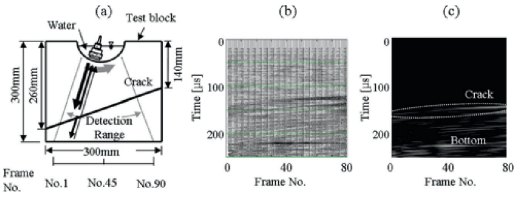

Figure 8. Rotating scanning test for a plaster with crack: (a) Test setup; (b) A-mode image; (c) B-mode image.

to form the concave shape for the rotational scanning, as shown in Figures 7–9. Water, which was filled in the concave part of the plaster block, was used as the coupling layer.

Intact Plaster Block. The rotational scanning tests on the intact block were carried out, as shown in Figure 8(a). The rotational scanning test on an intact plaster block clearly shows the interface at the bottom of the plaster block as shown in Figures 7(b) and (c). The brightest part in the B-mode occurred in the middle of the bottom. Because the reflected signal at the bottom of the plaster block was trapped in the water coupling layer, the signals with the intermediate amplitude were also detected below the bottom of the plaster.

Plaster Block with an Inclined Crack. After the intact plaster block was cut into two parts in the inclined direction as shown in Figure 8(a), the two parts were filled with thin vacuum grease to maximize the energy transmitted through the crack. The result of the rotational scanning test is shown in Figures 8(b) and (c). Two strong reflected signals were detected from the inclined crack and from the bottom of the block, respectively. The first strong reflection occurred at the inclined crack. Note the inclination of the crack was observed in the B-mode. The amplitude or the brightness of the reflected signals increases as the angle of incidence of the transducer beam becomes zero degree with the normal to the crack (right side). Note the brightest part in the B-mode corresponds to the strongest reflection from the discontinuity, which is perpendicular or normal to the transducer. Therefore, the brightest section can be used to determine the angle of the inclined discontinuity. In addition, because the reflected signal at the inclined crack was also trapped in the water coupling layer, the multiple reflections were observed. Note the inclination in the

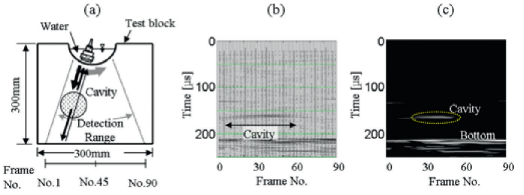

Figure 9. Rotating scanning test for a plaster cavity: (a) Test setup; (b) A-mode image; (c) B-mode image.

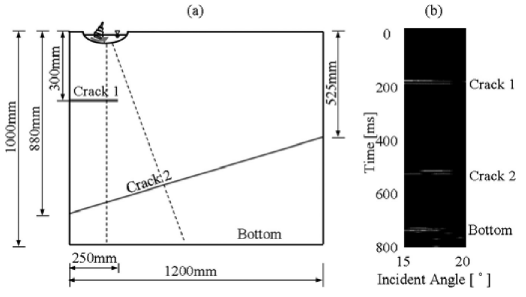

Figure 10. Rotating scanning test for a large scale plaster block: (a) Test setup; (b) B-mode image.

multiple reflections was identical with that of the first reflection, which came from the inclined crack. The second strong reflection was measured at the middle of the bottom of the plaster block because the angle of the incident wave became zero with the normal to the bottom of the plaster block.

Plaster Block with a Cavity. A hole (Diameter = 30 mm) was drilled on the intact block, as shown in Figure 9(a). The results of the rotational scanning test are plotted in Figures 9(b) and (c). Strong signals were also reflected from the bottom. The estimated diameter of the cavity from the B-mode was about 43 mm. Note, the difference between the real size (30 mm) and the estimated size (43 mm) results from the divergence of the beam, Fresnell's ellipse, and the transducer size. Although the inclined crack produced a continuous reflection line as shown in Figure 8(c), the cavity only yielded the reflections in a limited range. Furthermore, the amplitude of the image from the cavity decreased when the angle of the incident waves diverted from the normal to the cavity.

4.2 *Rotating scanning test for a large scale plaster block*

The dimensions of the large scale plaster block were 1000 mm in height, 1200 mm in width and 150 mm in thickness. For the rotational scanning test, the left part of the top surface of the plaster block was dug to form the concave shape, and water was filled, as shown in Figure 10. The rotational interval was 0.5 degree, which corresponded to 8.7 mm horizontal displacement at the bottom of the large scale plaster

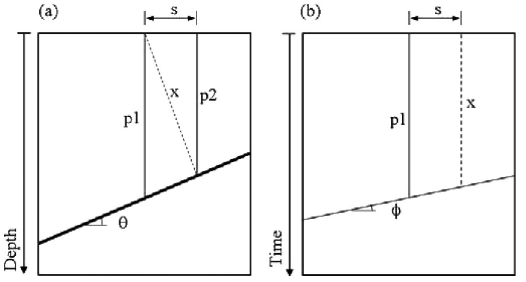

Figure 11. Effect of inclination angle: (a) Real discontinuity; (b) Ultrasonic reflection image.

block. To simulate the multiple discontinuities, two discontinuities were prefabricated: one was horizontal, and the other was inclined. The first horizontal crack whose gap and length were about 10 mm and 250 mm was filled with very weak and low viscous plaster paste for partial transmission and reflection of the ultrasonic waves at this discontinuity. The second long and inclined crack was filled with vacuum grease. B-mode is represented in Figure 10(b), that shows clear reflections from the first horizontal crack and the second inclined crack. In addition, the bottom of the plaster block could be identified, even though it was not clear.

5 DISCUSSION

5.1 *Inclination angle of images*

The inclination angle of the reflected image from the crack was flatter than that from a real crack, as shown in Figure 8. The relationship of the inclination angle between the reflected image ϕ and the real discontinuity θ is

$$\tan\varphi = \frac{p_1 - \sqrt{s^2 + p_2^2}}{p_1 - p_2}\tan\theta \qquad (4)$$

where, p_1 and p_2 are the depths of the discontinuity at two points separated by the horizontal distances (see Figure 11), and note, p_1 in the reflected image is the travel distance based on the travel time and velocity of the ultrasonic wave. The inclination angle of the discontinuity estimated by Equation (4) may be confirmed by the strongest brightness in the B-mode (see Figure 8).

5.2 *Horizontal scanning versus rotating scanning*

After a paraffin block was installed underwater, typical horizontal scanning (see details in Lee and Santamarina 2005) and rotating scanning tests were carried out. The experimental setups are shown in Figure 12(a). The thickness of the paraffin was 35 mm. For the typical horizontal scanning test, the ultrasonic waves

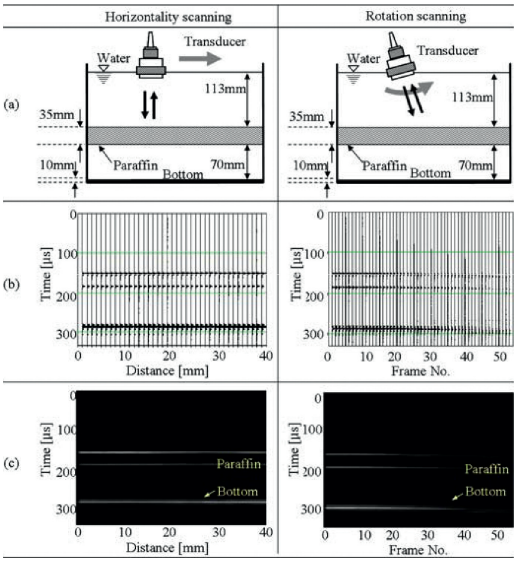

Figure 12. Comparison between rotating scanning and horizontal scanning tests: (a) Test setup; (b) A-mode image; (c) B-mode image.

reached perpendicularly to the interface. That is, the angle of incidence of the transducer beam was always zero degree with the normal to the interface. Thus, only reflection and transmission occurred at the interface. The amplitudes of the reflected and transmitted waves depend on the impedance mismatch. The scanning interval was set to 1 mm to avoid spatial aliasing (wavelength in water is $\lambda = 3$ mm because the velocity of the ultrasonic waves in water is about 1500 m/s and the frequency of the transducer is 500 kHz). Note no migration processing was required because high directivity transducers were used (Figure 4). Horizontal scanning could clearly detect the horizontal paraffin wax layer in water. Furthermore, the bottom of the water box was also clearly seen, as shown in Figures 12(b) and (c).

For the rotating scanning test, the ultrasonic wave may reach non-perpendicularly to the interface, and therefore, a mode conversion may occur (see details in Richart et al. 1970; Aki and Richards 1980). As the angle of incidence of the transducer beam increases from zero degree as shown in Figure 12(a), the arrival time of the reflected wave increases, the amplitude of the reflected waves decreases and finally diminishes, as shown in Figures 12(b) and (c), for the rotating scanning test. However, B-mode obtained by the horizontal scanning and by rotation scanning is almost identical due to the size of the transducer (19 mm in diameter), divergence (see Figure 4), and Fresnell's ellipse. Note images obtained by horizontal scanning and rotating scanning techniques are related to the lateral resolution. Thus, the reflected waves are still measured even when the incident waves diverges from the normal to the interface.

6 CONCLUSIONS

The design and application of ultrasonic wave reflection imaging were documented in this study for the detection of the discontinuity planes or cavities in laboratory scale rock models. The signal processing, which includes stacking, signal compensation, demodulation, rectification, smoothing, and rejection, were carried out to produce the amplitude and brightness modes (As and B-modes). The main observations of this study follow:

Although vacuum grease transmits more energy to the medium tested, water is recommended as the coupling layer for the horizontal and rotating scanning techniques because constant contact area is maintained in water and the directly transmitted wave between transducers may be effectively removed.

The discontinuities of the plaster block, including horizontal and inclined cracks, and the cavity were clearly detected by using the new rotating scanning technique. While the horizontal and inclined cracks yielded continuous reflections, the cavity produced reflections at a limited zone. B-mode is more appropriate for the detection of discontinuities.

The paraffin wax underwater was clearly detected by the typical horizontal scanning and rotating scanning techniques. Furthermore, the two techniques produced almost identical images. However, cautions are required for the analysis of results obtained by the rotating scanning technique.

The angle of the inclination obtained by the rotating scanning technique may give the angle of the original inclined crack through the comparisons of brightness and through a simple calculation based on geometry.

REFERENCES

Aki, K. & Richards, P.G. 1980. *Quantitative Seismology – Theory and Methods* Vol. 1 and 2: 932. Freeman Company, San Francisco.

Gomm, T.J. & Mauseth, J.A. 1999. *State of the Technology: Ultrasonic Tomography, Materials Evaluation* Vol. 57: 737–755.

Krautkramer, J. & Krautkramer, H. 1990. *Ultrasonic Testing of Materials*: 677. Springer-verlag, London.

Lee, J.S. & Santanmarina, J.C. 2005. P-Wave Reflection Imaging. *Geotechnical Testing Journal* Vol. 28 : 197–206.

Richart, F.E., Hall, J.R. & Woods, R.D. 1970. *Vibrations of Soils and Foundations*: 414. Prentice-Hall, USA.

Schmmer, L.W. Jr. 1998. *Fundamentals of Ultrasonic Nondestructive Evaluation – A Modeling Approach*: 559 Plenum Press.

Wells, P.N.T. 1977. *Biomedical Ultrasonics*: 635. Academic Press, London.

Zagzebski, J.A. 1996. *Essentials of Ultrasound Physics*: 220. Mosby, Inc., Missouri.